Journal of the Korean Nuclear Society
Volume 33, Number 3, pp.283~297, June, 2001

Effect of Spacer Grids on CHF at PWR Operating Conditions

Seung-Hoon Ahn
Korea Institute of Nuclear Safety
19 Gusong-dong, Yusong-gu, Taejon, 305-600, Korea
k175ash@kins.re.kr
Gyoo-Dong Jeun
Hanyang University
17 Haengdang-dong, Sungdong-gu, Seoul 133-791, Korea
thlab@email.hanyang.ac.kr

(Received August 28, 2000)

Abstract

The CHF in PWR rod bundles is usually predicted by the local flow correlation approach based on subchannel analysis while difficulty exists due to the existence of spacer grids especially with mixing vanes. In order to evaluate the effect of spacer grids on CHF, the experimental rod bundle data with various types of spacer grids were analyzed using the subchannel code, COBRA-IV-i. For the plain grid data, a CHF correlation was described as a function of local flow conditions and heated length, and then the residuals of the CHF in mixing vaned grids predicted by the correlation were examined in various kinds of grids. In order to compensate for the residual, three parameters, distances between grids and from the last grid to the CHF site, and equivalent hydraulic diameter were introduced into a grid parameter function representing the remaining effect of spacer grids except mixing. The present CHF correlation for plain grids predicted most of the CHF data points in plain grids within ± 20 percent error band. Good agreement with the CHF data was also shown when the grid parameter function for mixing vaned grids of a specific design was used to compensate for the residuals of the CHF data predicted by the correlation.

Key Words : CHF, spacer grids, mixing, local flow condition, PWR, rod bundle, subchannel analysis

1. Introduction

A recognized operating limit on pressurized water reactors (PWRs) is the abrupt and dramatic degradation in heat transfer characterized by the departure from nucleate boiling (DNB) phenomenon. DNB causes the replacement of the liquid by the vapor adjacent to the heated surface. The vapor blanket acts as a barrier to heat flow from a heated rod, resulting in a very sharp

increase of the fuel rod surface temperature involving a possible deterioration of the cladding material. Therefore, a reliable prediction of the critical heat flux (CHF), which is defined as the maximum heat flux just before DNB, is of importance in the design and safety analysis of PWRs.

Of the approaches in predicting the CHF at the PWR operating conditions, the most preferred is the local flow correlation approach, where the empirical CHF correlation is applied to local flow conditions [1]. In order to obtain local flow conditions which are usually determined at the scale of a subchannel surrounded by 3 or 4 rods, a procedure described as "subchannel analysis" is generally used with help of the computer code implementing the procedure [2]. When determining the local flow conditions, the fine structures of enthalpy and mass velocity distribution within the individual control volumes are ignored. The interactions between the individual subchannels, which during computation are assumed to act as independent parallel channels, are taken into consideration by an appropriate mixing correlation with empirically determined constants.

There are two difficulties that lie in applying the subchannel analysis to PWR rod bundles due to the presence of spacer grids. The first is that the spacer grids increase flow resistance and turbulence which in turn promote mixing, thus reducing any flow and enthalpy imbalance between subchannels. Second, secondary flow vortices can be significantly developed by the spacer grids with mixing vanes, whose development enhances the agitation of the bubble layer on the rods, thus leading to a decrease in bubble layer thickness. In subchannel analysis, the former is often quantified by a mixing coefficient and incorporated in the local flow conditions predicted by the subchannel code, and the latter is directly taken into consideration by the correlation itself throughout evaluation of the CHF data. This approach is practically useful for obtaining an accurate correlation as long as used within applicable range of the correlation. In addition, an attention is drawn on the case where the latter effect becomes important to enhance DNB performance, resultantly the CHF prediction deviating significantly from the local condition hypothesis [3]. In this case, other geometric parameters in addition to local parameters are often introduced into the correlation itself, based on experimental observations. However, without enough experimental CHF data to identify the CHF dependency on the parameters, the incorrect correlation form, whose fallacy is concealed during correlation development, can be used to evaluate the PWR thermal margin.

This study is intended to present how the effects of spacer grids can be handled in determining the empirical CHF correlation for PWR rod bundles and to emphasize the importance of the correlation form in evaluating the thermal margin. By means of a literature survey, a correlation form, where the effect of local parameters and the remaining effect of spacer grids except mixing are decoupled, is proposed. The CHF correlation for plain grids is developed and used to evaluate the residuals of the CHF in mixing vaned grids predicted by the correlation. Application to the CHF data in mixing vaned grids of a specific design is also presented. Lastly, discussions are made on implication of different correlation forms in evaluating the thermal margin and on applicability of the proposed approach.

2. Review of Literature

There have been several attempts to indicate how the effect of spacer grids can be handled when applying the round tube CHF prediction

techniques to the rod bundles. Tong [5] applied his single-channel DNB correlation, W-3, to the prediction of CHF data obtained from rod bundles at low qualities, based on the premise that thermal hydraulic behavior in any one subchannel within a rod bundle is similar to that in a round tube. With other corrections such as cold wall and heat flux distribution effects, he found it necessary to multiply the W-3 predictions by a grid factor, F_s, which depends on the local mass velocity and thermal diffusion coefficient (*TDC*). In the evaluation it was implied that rod bundles with simple or plain grids (no mixing vanes) would not require use of the grid factor.

Extending Tong's study, Rosal, et. al. [6] investigated the effect on DNB from geometry of spacer grids (mixing vane or non-mixing vane) and axial grid spacing along the rod. It was noted that the mean of the measured-to-predicted CHF ratio for the shorter grid span DNB data was higher than that of the longer grid span data and the mixing vane gave a higher mean, even with the higher mixing coefficients. He also reported that the inner edge of any mixing vane is located very close to the heated rod and it peels off the bubbly layer, which shields the rod from being cooled by the main streamed liquid.

Other studies have also shown that DNB performance is typically better in mixing vaned grids than in plain grids and is improved as the distance between grids shortens [7,8]. These observations are also made in examination of the correlations, which have been directly developed from the CHF data in rod bundles. Typical of these correlations is the WRB-1 correlation which has been developed by F.E. Motley, et al. [9]. The correlation is said to provide an appreciably better fit of the CHF data in Westinghouse rod bundles with mixing vaned grids but the detailed form and coefficients of the correlation were not published for proprietary reason. H.B. Giap, et al. [10] also developed a correlation named as TUE-1 for the same types of Westinghouse rod bundles. Distance between grids, is involved in the correlation as one of independent parameters, in such a way that the CHF increases as it shortens. However, a quantitative effect of mixing vaned grids is not investigated in the correlation. Differently from these correlations, the CE-1 correlation, which has been developed by F.D. Lawrence [11], fit the CHF data for Combustion Engineering rod bundles with its standard spacer grids (without mixing vanes). Only the local flow conditions were taken into account in the correlation without use of any other parameters, such as heated length and distance between grids, etc.

Meanwhile, it has been reported [12,13] that the theoretical CHF prediction in round tubes could be successfully applied to that in rod bundles. Because they could not take into account the complex effects of the mixing vaned grids on the local fluid dynamics within the subchannel, the application was restricted to the plain grid data. Application of the theoretical models to the mixing vaned grid data would require a correction, as Lin, et al. [14] introduced a grid factor, for correlating mixing vaned grid data. Many facts about local flow phenomena within a subchannel are not yet satisfactorily understood. However, recent studies on turbulent flow behavior in a rod bundle provide some implications on the local fluid dynamics within a subchannel. Rehme [15] has made extensive review on secondary flows in rod bundles. From examination of many other experimental observations, he concluded that secondary flows do not contribute significantly to the mixing between subchannels of rod bundles since the secondary flow vortices are expected to move within the elementary cells of the subchannel. He also remarked that the main reason for the turbulent mixing between subchannels is due to periodical flow pulsation

between subchannels, not secondary flows.

In relation to the secondary flow behavior in a rod bundle, there was a noticeable indication of de Crecy [16] on the effect of mixing vaned grids. He split the total effect of spacer grids into a mixing effect and an intrinsic effect, when analyzing the effect of the mixing vanes on the CHF. The terminology, "intrinsic" is understood as "not quantified by subchannel analysis due to its intrinsic problem". He also concluded from analysis of his experimental results that the intrinsic effect may be either positive (benefits with mixing vanes) or negative (benefits without mixing vanes) and depends a great deal on the thermal hydraulic parameters such as pressure and mass velocity.

3. Rod Bundle CHF Data Analysis

3.1. Representation of Correlation form

A rod bundle CHF correlation is formulated by investigating the parametric effects on the CHF and then two groups of parameters are identified. One group of parameters is calculated by the subchannel code, for which the CHF is often expressed by the correlation with the form

$$q''_{p,1} = f(P, G_{loc}, \chi_{loc}; D_e), \quad (1)$$

where D_e often specifies the boundary where the local condition hypothesis is valid. The heated length, L_H is additionally taken into account in some cases. The other group is introduced to compensate for the remaining effects, which are not quantified by subchannel analysis. The remaining effects involve cold wall, heat flux distribution, and spacer grid effects [17]. So far as the spacer grid effect is concerned, the CHF effect is dependent largely on the degree that a grid design contributes to improvement of secondary flow vortices. If they are improved, stronger hydrodynamic force will act on the bubbly layer near the hot rod, retarding the bubble coalescence from reaching a critical point where CHF occurs. In a usual grid configuration, longer distance between grids is less effective for improvement of secondary flow vortices than shorter because most of them will be merged into the main streamed flow before reaching the next grid. It is similar in case of distance from the last grid to the CHF site. Another consideration is the subchannel size, specified by D_e, from intuitive reasoning that the larger D_e goes, the weaker hydrodynamic force will act on the bubbly layer near the rod even for the same distances between grids and from the last grid to the CHF site. Then, the CHF effect induced by spacer grids can be represented by a grid parameter function with the form

$$q''_{p,2} = g(d_{g-g}, d_{g-c}, D_e; \varphi), \quad (2)$$

where φ designates the design character of spacer grids, which may be represented by the presence of mixing vanes, and their position, dimension, shape and inclination at the upper part of the spacer girds. There can be dependency of the heat flux, $q''_{p,2}$ on the thermal hydraulic parameters, which is not taken into account here for simplicity.

The intent to decouple the two CHF effects in a correlation form, e.g., effects represented by local and grid parameter functions, is to quantify more explicitly the remaining effect of spacer grids except mixing. The remaining portion, which the CHF is not described by one heat flux, $q''_{p,1}$, will be taken charge of by the other heat flux, $q''_{p,2}$ by the residual δ defined as

$$\delta = q''_m - q''_{p,1} \quad (3)$$

This decoupling is similar to the use of a grid factor in applying the round tube CHF prediction

Table 1. Characteristics of Selected Test Sections

Rod Arrangement	5×5 rod arrays with matrix subchannels 21 rods with one large unheated rod 4×4 rod arrays with matrix subchannels*
Equivalent hydraulic diameter (*De*)	1.178 to 1.354 cm
Rod diameter (*DR*)	0.914 to 1.118 cm
Distance between grids (d_{g-g})	30.48 to 66.04 cm
Rod to wall gap	0.249 to 0.508 cm
Heated length (L_H)	1.83 to 3.81 m
Grid type	plain or mixing vane grids with C_g=0.635 to 1.820
Axial heat flux distribution	uniform (and non-uniform)

* test section of mixing vaned grids and non-uniform axial heat flux distribution

Table 2. Major input options of COBRA-IV-i

Input correlation options	Value or Correlation
Subcooled void	Levy model
Bulk void fraction	Modified Armand correlation
Two-phase friction multiplier	Armand correlation
Turbulent mixing correlation	$W_{ij}=\beta s G_{loc}$
Single-phase friction factor	$f=0.184Re^{-0.2}$
Cross flow resistance factor	0.5
Cross flow momentum factor	0.5

technique to rod bundles, but more advantageous for precisely evaluating the parametric effects of d_{g-g} and d_{g-c} over the entire parameter range.

3.2. Data Selection and Subchannel Modeling

Data is available for analysis of the rod bundle CHF, which is compiled of extensive data of the CHF tests carried out at Columbia University [18]. Only the limited number of the data has been selected at the test bundles whose conditions are representative of the PWR operating conditions. Each test bundle is basically composed of a 5x5 rod array or its equivalent with uniform axial heat flux distribution. The CHF data at the test bundles with 4x4 rod arrays are also available but used only when the CHF data of 5x5 rod array are deficient as seen in case of the mixing vane grid data. Characteristics of the selected test sections are described in table 1.

Multiple CHF indications were observed in most of the selected data. Only the first CHF indication except on peripheral rods is used for the henceforth CHF data analysis, e.g., the measured local heat flux at the experimental location of the first CHF indication is compared with the predicted CHF calculated using local conditions from subchannel analysis. Additionally, for CHF indications on interior heater rods with single thermocouple instrumentation, it is assumed that CHF initiates in the matrix subchannel with the highest predicted local quality at the CHF site.

A thermal-hydraulic subchannel analysis code, COBRA-IV-i is used to obtain the local flow conditions at the measured CHF site. The major input options of the computer code chosen for this study are summarized in table 2. Although

Table 3. W-3 Prediction Results for Selected Data in Its Applicable Range

Cg	dg-g, cm	no. of data	$\frac{q''_{m,ave}-q''_{p,ave}}{q''_{m,ave}}$, %	$\overline{X}(R)$	$S(R)$
0.635	39.4	32	-11.8	0.91	0.126
0.700	38.1	47	32.0	1.51	0.275
0.815	36.3 to 46.5	294	-9.2	0.94	0.183
1.018	36.3 to 44.2	46	-10.1	0.95	0.249

various input options provided by this computer code generally rely on the test conditions, no other options but turbulent mixing have significant effects on determination of local flow conditions in PWR operating conditions [19]. The value of a mixing coefficient, β (often called mixing Stanton number) used in the turbulent mixing correlation varies as flow boiling regions as well as grid designs. Because of deficiency of reliable experimental values for the two-phase flow representative for a CHF condition, the single-phase mixing coefficient is usually used. In this study, the value of β, 0.02 was used for plain grids and 0.06 for mixing vaned grids. The effect of β on the CHF prediction is discussed in 4.2.3.

3.3. Determination of Correlation for Plain Grids

In advance of determining the correlation for plain grids, it is necessary to select the test sections where thermal hydraulic behavior in any one subchannel is the most similar to that in a round tube. A well known round tube correlation, the W-3 correlation [5] was used to calculate the ratio R, which is defined as

$$R = \frac{q''_m}{q''_p}. \quad (4)$$

If the mean of R, $\overline{X}(R)$ becomes close to unity in a test bundle with plain grids by using W-3, it is presumed that an appropriate form of the local parameter function of eq.(1) will provide a good fit of the CHF data in the test bundle. Only the data where the CHF initiated in the matrix subchannel (without cold wall) was used to calculate the ratio R. Table 3 shows that the CHF tends to be a little over-predicted by W-3 except that with C_g=0.700 (TS 405). Considering that TS 405 has smaller rod-to-wall gap spacing and experiences higher CHF values compared to those with other plain grids, the CHF data can be dismissed from this CHF analysis. The CHF data of C_g=0.815 and C_g=1.108 were selected for determination of the correlation for plain grids, because the number of data points are relatively abundant and the means of the ratio R are closest to unity. A form of the local parameter function depends on the experimental observation of the relationship between the CHF and the independent parameters. For simplicity the local condition form of the generalized EPRI-1 correlation [21] was used:

$$f = (A' - x_{loc})/C', \quad (5)$$

where A′ and C′ are the unspecified functions dependent on P, G_{loc}, and D_e. The functional forms of A′ and C′ were also assumed to be the same as those used in EPRI-1, which were originally proposed by Macbeth [22]. A regression analysis is usually employed to obtain the coefficients of the function that correlate the

Table 4. One-way Analysis of Variance for Local Parameter Function Without Heated Length

Test sections	No. of data	$\overline{X}(R)$	$S(R)$	t-value from t-test	F-value from F-test
TS 21.0,36.1,48.0,52.0	270	1.023	0.0841	6.942	48.191
TS 38.0, 47.0	111	0.955	0.0915		

Table 5. Optimized Coefficients of Local Parameter Function and Its Applicable Range

Coefficients	Values	Coefficients	Values
a_1	0.45949	a^6	-0.19853
a_2	-0.08152	a^7	0.12945
a_3	1.33586×10^{-4}	a^8	-0.32506
a_4	0.89475	a^9	0.30715
a_5	-0.59533	a^{10}	0.52161

Regression range for each parameters

Pressure	9.6 to 16.6 MPa,
Local mass velocity	1.22×10^3 to 5.42×10^3 kg/m^2 sec
Local quality	-0.1 to 0.2
Heated length	2.13 to 3.81 m

Statistics of the ratio R

Test sections	No. of data	$\overline{X}(R)$	$S(R)$
Total	381	1.002	0.0856
21.0	42	1.018	0.0992
36.1	79	0.990	0.0802
38.0	43	1.019	0.0840
47.0	68	0.971	0.0932
48.0	80	1.036	0.0826
52.0	59	0.978	0.0587

independent and dependent parameters [23]. The correlation, which was determined through the regression analysis, was used to calculate the ratio R for each CHF data which was rearranged for subsets of the CHF data with different heated lengths and/or grid loss coefficients. As shown in table 4, the results of the F and t-tests [24] indicate that there is a statistically dependence on the heated length. After extensive trial and error fitting, it was concluded that a parameter, heated length should be considered additionally to the power function of G for A' and C'. Then the

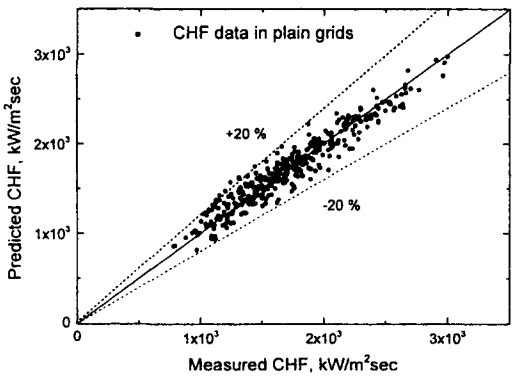

Fig. 1. Measured Versus Predicted CHF for the Plain Grid Data Using Local Parameter Function

correlation for plain grids is expressed by the following local parameter function:

$$f = \frac{a_1 \tilde{P}_r^{\,a_2} \tilde{G}_{loc}^{\,a_3+a_7\tilde{P}_r+a_9\tilde{L}_r} - x_{loc}}{a_3 \tilde{P}_r^{\,a_4} \tilde{G}_{loc}^{\,a_6+a_8\tilde{P}_r+a_{10}\tilde{L}_r}}, \qquad (6)$$

where a_1, a_2, ··· a_{10} correlation coefficients and the hyphens represent conversions of the SI units to the British units, which were used for regression analysis, e.g., $\tilde{P}_r = P_r/0.006894$, $\tilde{G}_{loc}/1356.23$, $\tilde{L}_r = L_r/0.0254$. Table 5 summarizes the result of the regression analysis which has been used to obtain the values of coefficients, a_1, a_2, ···a_{10}. Statistics for the ratio R in this table demonstrate that the correlation represented by the local parameter function of eq. (6) provides good prediction of the CHF in plain grids without biased prediction to any particular data groups. Comparison of the predicted and measured CHF values is presented in fig. 1. As can be seen, most of the data points fall within ±20 percent error

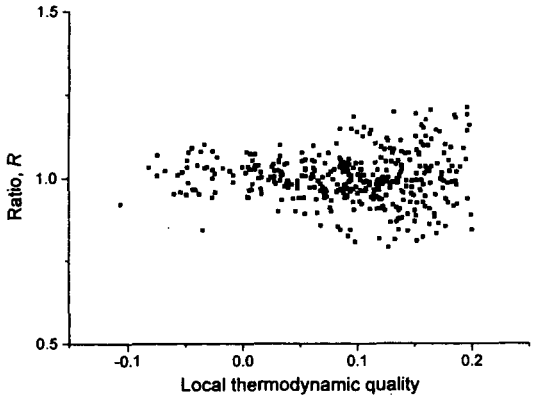

Fig. 2. Variation with Local Thermodynamic Quality of Ratio *R* Using Local Parameter Function

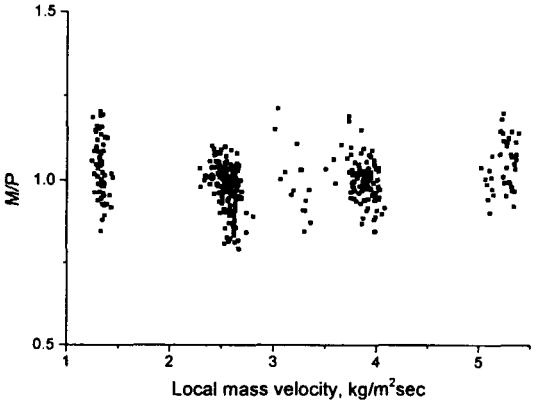

Fig. 3. Variation with Local Mass Velocity of Ratio *R* Using Local Parameter Function

band. The performance of the correlation on the variation of local parameters was also investigated, and no significant bias was found, as seen in figures 2-4.

3.4. Evaluation of Grid Effect on the CHF

The relative effect of mixing vaned grids against plain grids can be evaluated by investigating the residual of the CHF in mixing vaned grids predicted by eq.(6). The CHF data in mixing vaned

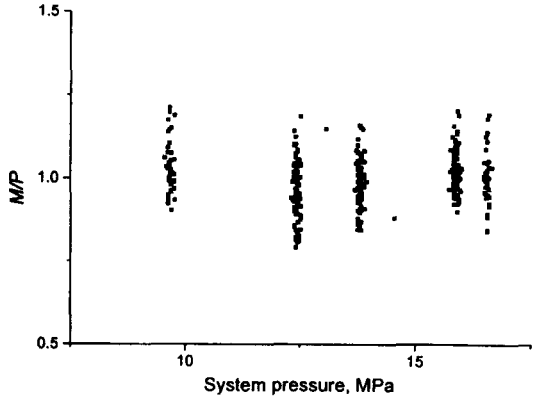

Fig. 4. Variation with System Pressure of Ratio *R* Using Local Parameter Function

grids were selected from test sections of C_g=1.250 (TS 157, 160, and 163), C_g=1.484 (TS 31 and 34) and C_g=1.820 (TS 140 and 141). The CHF in mixing vaned grids of C_g=1.820 (TS 140 and 141) was measured at test bundles of 4×4 rod arrays with non-uniform axial heat flux distributions. The CHF locations of the test bundle were measured by 6 thermocouples positioned at the upstream of spacer grids and between spacer grids. In some test runs, the CHF occurred first at the thermocouples positioned at the just upstream of spacer grids, but first at those between spacer grids in other runs. In order to compensate for the heat flux distribution effect, Tong's non-uniform factor, F [17] was applied by modifying the residual δ of eq.(3) to

$$\delta = Fq''_m - q''_{p,l} \cdot \qquad (7)$$

Figure 5 shows the residual δ in mixing vaned grids against the sum of $d_{g\text{-}g}$ and $d_{g\text{-}c}$ divided by D_e. For comparison, the residual δ in plain grids of C_g=0.815 and 1.018 are also presented in the figure. A general trend is observed that the smaller $d_{g\text{-}c}$ or $d_{g\text{-}g}$ goes, the larger the residual δ gets. In C_g=1.484, the residual δ for shorter $d_{g\text{-}g}$ is larger

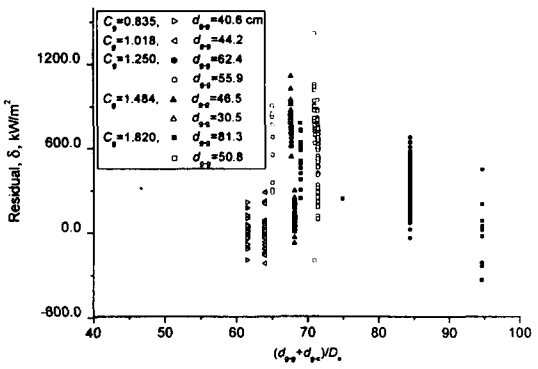

Figure 5. Comparison of Residual δ for the CHF Data in Various Grid Designs

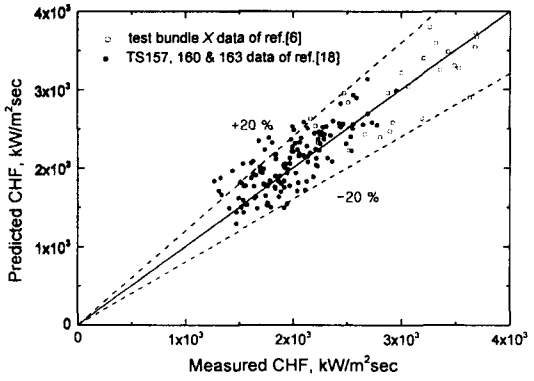

Fig. 7. Predicted Versus Measured CHF in Westinghouse Mixing Vaned Grids

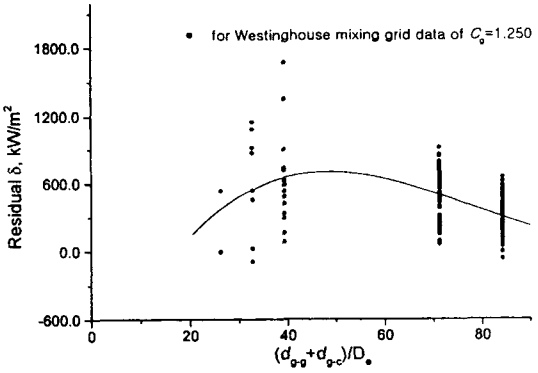

Figure 6. Dependency of Residual δ on the Sum of $d_{g\text{-}g}$ and $d_{g\text{-}c}$ in Westinghouse Mixing Vaned Grids

than that for longer $d_{g\text{-}g}$, at almost the same values of the sum of two distances, e.g.,$(d_{g\text{-}g}+d_{g\text{-}c})/D_e \approx$ 68. Comparing the cases of C_g=1.484, $d_{g\text{-}g}$=30.5 cm and C_g=1.820, $d_{g\text{-}g}$=50.8 cm, it is also shown that the residual δ for the former case with a larger value of $(d_{g\text{-}g}+d_{g\text{-}c})/D_e$ is larger than that for the latter case. Thus, it seems that the residual δ depends more strongly on $d_{g\text{-}g}$ than on $d_{g\text{-}c}$, Moreover, the effect of $d_{g\text{-}g}$ increases dramatically at shorter distance between grids.

Because the mixing vaned grid data are rare especially for the shorter distance between grids, it is impossible to determine the complete form of the grid parameter function, g of eq. (2) with the currently selected data only. To simplify our study, an effort was made to determine the grid parameter function for the mixing vane grid data with loss coefficient of C_g=1.250, where the effects of $d_{g\text{-}g}$ and $d_{g\text{-}c}$ on δ do not appear very differently. The CHF data for smaller $d_{g\text{-}g}$, 25.4 cm, was additionally selected from ref. [6], where the test bundle X is composed of a 4×4 rod array, top-skewed axial heat flux distribution. Figure 6 shows the residual δ, which are calculated for each CHF within the applicable parameter range of the correlation for plain grids. The following least-square fitting curve of the residuals was obtained:

$$g = -1233.25 + 93.94\left[(d_{g\text{-}g} + d_{g\text{-}c})/D_e\right] - 1.41\left[(d_{g\text{-}g} + d_{g\text{-}c})/D_e\right]^2 + 0.0061\left[(d_{g\text{-}g} + d_{g\text{-}c})/D_e\right]^3 \quad (8)$$

If this grid parameter function is used to compensate for the residual of the CHF predicted by the correlation for plain grids, most of the predicted CHF corresponds to the measured CHF within 20 percents, as plotted in fig. 7. In order to obtain more precise form of the grid parameter function, additional CHF data is to be available for

Table 6. Statistics of Ratio of the Measured and Predicted CHF in Westinghouse Mixing Vaned Grids

Correlations	No. of data	$\bar{X}(R)$	$S(R)$
Original W-3	92	1.180	0.1868
W-3 × F_s	105	1.059	0.1545
W-3 × $F_{s,L}$	92	1.034	0.1020
Proposed correlation (q''_p=f+g)	164	1.002	0.0999
q''_p × $F_{s,L}$	164	1.178	0.1472

public use.

The accuracy of CHF prediction by the proposed correlation was also compared with that of the round tube correlations or with some corrections. As seen in table 6, the CHF in mixing vaned grids is better predicted by the proposed approach. In this comparison, R statistics for each correlation were obtained within its applicable range.

4. Discussions

4.1. Implication of Correlation Form

The usual approach for evaluating the PWR thermal margin is recalled in order to investigate implication of the correlation form in evaluating PWR thermal margin. The CHF margin, $\delta q''$ is defined as

$$\delta q'' = q''_c - q''_{loc}, \qquad (10)$$

where q''_c and q''_{loc} are the critical heat flux and the local heat flux at the hottest rod in the actual core respectively. In the current PWR design it is usually assumed that an experimental CHF testing reflects the reality of the DNB in the actual core: that is, $q''_c = q''_m$. In this case a percent thermal margin is obtained by dividing two sides of eq. (10) by the measured CHF.

$$\delta q'' / q''_m = 1 - \frac{1}{R}\frac{1}{DNBR}, \qquad (11)$$

where $R=q''_m/q''_p$ and DNBR is usually defined by q''_p/q''_{loc}. Traditionally the DNBR has been used as an indicator of the thermal margin in PWR. For example, a conventional design requires that DNBR at the hottest rod during normal operation and anticipated transients be above the specified tolerance limit of the reciprocal of R, so called the correlation DNBR limit. In order to maximize the thermal margin, the desire is to establish the correlation with high accuracy for a particular fuel and to minimize the amount of margin which must be set aside to cover the uncertainty of the correlation.

The question is raised on whether a credit of the correlation performance can be taken only by investigating R or DNBR statistics. Thus, the following two cases were evaluated and compared when predicting the CHF data in one test bundle with mixing vaned grids (TS 157) included in this study.

a) Predicted by the proposed correlation, e.g., $q''_p = f+g$, and

b) Predicted only by a form of the local parameter function, e.g., $q''_p = f^*$.

Regression analysis was performed for each case. Table 7 shows comparison between statistics of the ratio R in two cases. The adjusted coefficients of f^* in case (b) are also included in the table. The ratio R in case (b) is less scattered than that in case

Table 7. Comparison of *R* Statistics and Adjusted Coefficients for a Local Parameter Function

Correlated functions	$\overline{X}(R)$	$S(R)$
Proposed correlation ($q''_p=f+g$)	1.012	0.0857
$q''_p=f^*(P, G, x)$	1.000	0.0631
Optimized coefficients of f^*		
a_1 = 0.97150, a_2 = -0.83684, a_3 = 0.87148, a_4 = -0.12049, a_5 = -0.15833, a_6 = -0.18102, a_7 = 0.60479, a_8 = -0.45116, a_9 = 0.15729, a_{10}= 0.47581		

* For TS 157 CHF data with number of 63

(a). If the standard deviations of the two are simply compared, it may be concluded that the correlation in case (b) leads to be more reliable than that in case (a). In order to reveal the fallacy of this conclusion, the CHF curves for the above two cases were linearly interpolated against local quality, assuming that P and G_{loc} are fixed at CHF conditions of a test run with no. 17. It is shown in fig. 8 that the DNBR sensitivities to the local quality are significantly different in two cases. The sensitivity becomes larger in case (b), where a grid effect is not quantified in the correlation itself but is compensated for by the effect of local parameters. The results are the same for other test conditions, as expected in two correlation forms.

If written in a more generalized manner, the following formulation is possible:

$$q''_p = Aq''_{p,1} + Bq''_{p,2} \qquad (12)$$

where the first and second terms of the right hand side denote dependency on local parameters and the remaining grid effect grid except mixing respectively. Because case (a), e.g., A=1 and B=1, reflects the reality in our study, the first term is determined so that:

$$A = (1 + (1 - B)q''_{p,2} / q''_{p,1}). \qquad (13)$$

If the grid effect is underestimated (B<1), the DNBR sensitivities on the parameters become

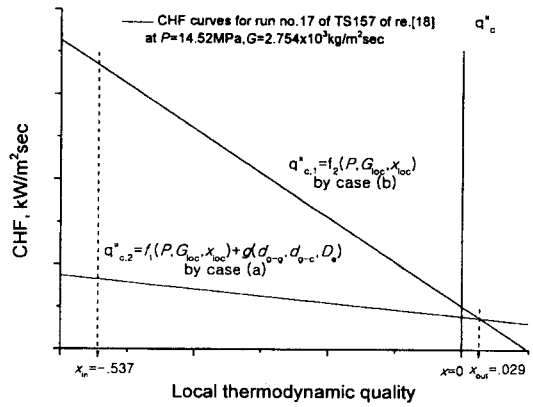

Figure 8. CHF Curves Versus Local Quality at Fixed Exit Condition

higher. On the contrary, if B>1, they will be lower. However, R or DNBR statistics tends to lose credibility in any cases where the grid effect is incorrectly evaluated; the accuracy of the correlation in case (b) will be decreased if more data are taken from other experiments.

4.2. Applicability of the Proposed Approach

4.2.1. Evaluation of Other Plain Grid CHF Data

In order to confirm the validity of the correlation for plain grids, e.g., eq. (6), it is necessary to examine the performance against other CHF data. The CHF data selected are taken from three test

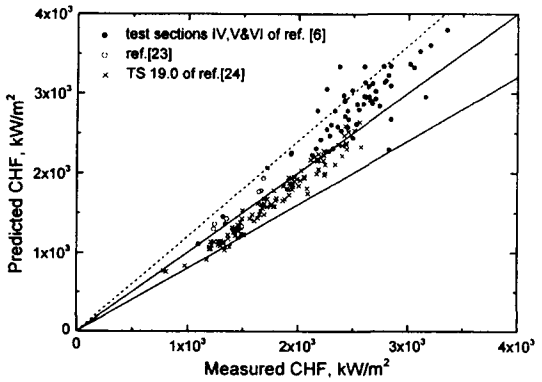

Fig. 9. Predicted Versus Measured CHF for the Plain Grid CHF Data

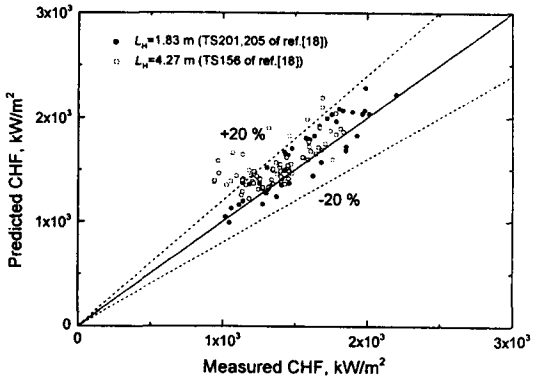

Fig. 10. Predicted Versus Measured CHF for Data with Heated Length Beyond Regression Range

bundles with plain grids:

(a) Three are in 4×4 rod array with heated 96 inch lengths and usineu axial heat flux distribution (test sections Ⅳ, Ⅴ, Ⅵ of ref.[6]),

(b) One is in a 5×5 rod array with a heated 118 inch length, uniform axial heat flux distribution and 0.12 inch rod-to-wall gap (a test section of ref.[23]), and

(c) The other is in a 5×5 rod array with a heated 118 inch length, uniform axial heat flux distribution and 0.14 inch rod-to-wall gap (a test section 19.0 of ref.[24]).

Configurations of test bundles (b) and (c) are very similar, although there are small differences of rod-to-wall gaps and radial power distributions. The test bundles of (a) are very different from two test bundles of (b) and (c). Beside use of smaller array, their rod diameter and pitches are 0.422 and 0.507 inches larger compared with 0.374 and 0.500 inches of (b) and (c). Figure 9 compares the predicted and measured values. As can be seen, some deviations in data of test bundle (a) reflect the increased CHF uncertainty due to smaller test bundle array, etc., while the proposed correlation provides good prediction with the CHF for designs of different origin. It implies that the CHF in plain grids is not significantly affected by spacer grid designs and a CHF correlation can be generalized to various plain grid designs, only if the correlation is applied to the range of PWR operating conditions.

4.2.2. Heated Length Effect

In this study, a modification of the local condition form of the generalized EPRI-1 correlation was made by additionally considering heated length because the CHF dependency on heated length was weak but not negligible. In a strict manner, it is inconsistent with the local condition hypothesis, which have been used extensively and successfully for correlating the round tube CHF data. In order to confirm deviations of the hypothesis which have been often observed in rod bundle CHF data analysis, the data of test bundles with heated length beyond the present regression range ($2.13 < L_H < 3.81$ m) were assessed. The selected test bundles are TS 201, 205 with plain grids and TS 156 with mixing vaned grids. As plotted in fig. 10, the CHF data with 1.83 m heated length is well predicted by the present while those with 4.27 m heated length tend to be over-predicted by the correlation for mixing vaned grids ($f+g$). This indicates that at the

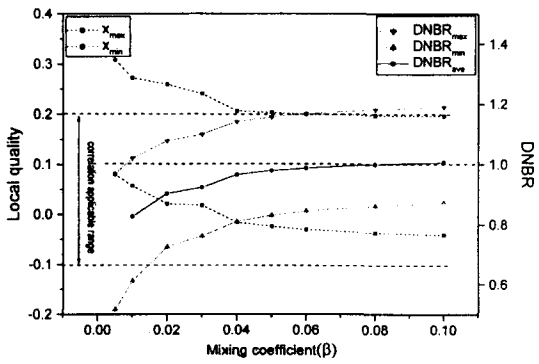

Fig. 11. Variation of Local Quality and DNBR Versus a Mixing Coefficient

same local flow conditions a rod with longer heated length experiences the CHF faster than other rods with shorter heated length. Thus, a CHF correlation must be used within the specified regression range of heated length.

4.2.3. Effect of Mixing Stanton Number

The value of a mixing coefficient, β, is highly dependent on the shape of the bundle and is usually determined through the thermal mixing test mostly for a single-phase flow. Because this study applied the roughly estimated value of β to mixing vaned grids, the effects of β on prediction of local quality and DNBR have been investigated for a rod bundle, TS 157. As shown in fig. 11, the predicted local quality decreases while the predicted DNBR increases, as the value of β increases. The variations of the two are very significant at the values of β less than 0.02, and are negligible more than 0.05. Especially, the prediction capability of the correlation is not largely affected even for high thermal mixing rate ($\beta \sim 0.1$). Thus, it is concluded that the value of β, 0.06 is appropriate for predicting the CHF in mixing vaned grids of this study without inducing a serious error.

5. Conclusions

In this study, an approach to handle the effects of spacer grids in determining the empirical CHF correlation for PWR rod bundles was proposed. A CHF correlation for plain grids was developed, which predicted the CHF data compared at this paper within ±20 percent error band. By introducing a grid parameter function to compensate for the residuals of the CHF values in mixing vaned grids of a specific design predicted by the correlation, good agreement with the CHF data was also shown at almost the same accuracy level as that in plain grids. These results indicate that decoupling of the two effects on the CHF in a correlation, the local parameter effect and the remaining effect of spacer grids except mixing, is efficient for quantifying the effects of spacer grids on the CHF and predicting the CHF in mixing vaned grids.

Recommendations for further study are as follows:

a) A more generalized CHF correlation needs to be developed for various plain grids, which can be used to evaluate the thermal margin improved by the fuel design change of plain to mixing vaned grids.

b) An effect on the local fluid dynamics or the CHF by presence of the grid just downstream of a mixing vaned grid should be investigated because, in some examples of our study, distance between grids has relatively more significant effect on the CHF than distance to the CHF site from the last grid, downstream of which no grid is present.

c) Parametric dependencies on the remaining effect of spacer grids except mixing should be more investigated because the present grid parameter function is based on the restricted database. More CHF data should be available in order to quantify the grid effect by using the

geometric and thermal hydraulic parameters.

Nomenclature

C_g	grid loss coefficient
D_e	hydraulic equivalent diameter (cm)
$d_{g\text{-}c}$	distance from the last grid to CHF site (cm)
$d_{g\text{-}g}$	distance between grids (cm)
F	Tong's non-uniform factor
G	mass velocity (kg/m^2 · sec)
L	heated length(m)
L_r	reduced heated length(=L/10^2)
P	system pressure (MPa)
P_r	reduced system pressure(= P/10^3)
q''	heat flux (kW/m^2)
R	ratio of measured and predicted CHF
s	gap spacing,
TDC	thermal diffusion coefficient (=β)
S(R)	standard deviation of R
W_{ij}	diversion cross flow per unit length (kg/m · sec)
X(R)	mean of R

Greek Symbols

x	thermodynamic quality
δ	residual of measured minus predicted CHF
β	mixing Stanton number (=$W_{ij}/G_{loc}s$)

Subscripts

c	critical heat flux condition
m	measured value of CHF
p	predicted value of CHF
loc	local condition

References

1. D.H. Hwang, et al., Development of a rod bundle correction method and its application to predicting CHF in rod bundles, Nucl. Engrg. & Des. 139, 205-220 (1993).
2. J. Weisman, Methods for detaile d thermal and hydraulic analysis of water-cooled reactors, Nucl. Sci. & Engrg., 57, 255-276 (1975).
3. P.G. Barnett, An investigation into the validity of certain hypotheses implied by various burnout correlation, U.K. AEA report, AEEW-R214 (1963).
4. C.L. Wheeler, et al., COBRA-IV-I: An interim version of COBRA for thermal hydraulic analysis of rod bundle nuclear fuel elements and cores, BNWL-1962, (1976).
5. L.S. Tong, An evaluation of the departure from nucleate boiling in bundles of reactor fuel rods, Nucl. Sci. Engrg. 33, 7-15 (1968).
6. E.R. Rosal, et al., High pressure rod bundle DNB data with axially non-uniform heat flux, Nucl. Engrg. & Des. 106, 209-220 (1974).
7. J. Yates, K. Galbraith, and R. Collingham, DNB and post-DNB heat transfer data in 25 rod bundles, XN-75-54, Exxon Nuclear Corp. 1975, presented at 3rd Water Reactor Safety Information Mtg. Washington, D.C., Sep. (1975).
8. D.C. Groeneveld and W.W. Yousef, Spacing devices for nuclear fuel bundles: A survey of their effect on CHF, Post-CHF heat transfer and pressure drop, ANS/ASME Int. Topl. Mtg. Nuclear reactor thermal-hydraulics, Saratoga, Springs, N.Y., Oct. (1980).
9. F.E. Motley, et al., New Westinghouse correlation WRB-1 for predicting critical heat flux in rod bundles with mixing vane grids, Westinghouse report, WCAP-8263, (1976).
10. H.B. Giap, et al., A new methodology for developing an empirical DNB correlation.
11. F.D. Lawrence, et al., Critical Heat Flux in PWR fuel assemblies, AIChE-ASME Heat Transfer Conf., Salk Lake City, Utah, Aug. 15-17 (1977).
12. J.C.M. Leung and R.E. Henry, Prediction of CHF in rod bundles using round tube CHF correlation, ANS Trans. 33, 963-966 (1979).

13. J. Weisman and S.H. Yang, A theoretically based in critical heat flux prediction for rod bundles at PWR conditions, Nucl. Engrg. & Des. 85, 239-250 (1985).
14. W.S. Lin, et al., "Bundle critical power predictions under normal and abnormal conditions in pressurized water reactors, Nucl. Tech. 98, 354-365 (1992).
15. K. Rheme, The structure of turbulence in rod bundles and the implications on natural mixing between the subchannels, Int. J. Heat Mass Transfer, 35, 567-581 (1992).
16. F. de Crecy, The effect of grid assembly mixing vanes on critical heat flux value and azimuthal location in fuel assemblies, NURETH-6, Grenoble (1993).
17. L.S. Tong, "Boiling crisis and critical heat flux," U.S. AEC. TID-25887 (1972).
18. D.G. Reddy and C.F. Fighetti, Parametric study of CHF data Vol.3: Critical heat flux data, EPRI-NP-2609 (1982).
19. D.G. Reddy and C.F. Fighetti, Parametric study of CHF data Vol.2: A generalized subchannel CHF correlation for PWR and BWR fuel assemblies, EPRI-NP-2609, (1982).
20. R.V. Macbeth, Burnout analysis, Part 4: Application of a local condition hypothesis to world data for uniformly heated round tubes and rectangular channels, U.K. AEA report, AEEW-R267 (1963).
21. SAS user's guide: Statistics, version 5 edition, SAS Institution Inc. (1985).
22. L.C. Edwin, et al., Statistics manual, Dover Publications Inc., New York (1956).
23. F.H. Bowditch and D.J. Mogford, "An experimental and analytical study of fluid flow and critical heat flux in PWR fuel elements," UKAEA report: AEEW-R2050 (1987).
24. Vogel, Mixing input data for SIEMENS test sections used by MIX84 code until 1989, KWU B123/1989/e377 (1989).